

# A New Comparative Study of Radiometric Correction on Satellite Images Using Kalman Filter and Levenberg Marquardt Algorithm

**Priti Tyagi, Udhav Bhosle**

*PVPP College of Engineering, Rajiv Gandhi Institute of Technology, India*  
tpriti15@rediffmail.com, udhavgbhosle@gmail.com

## ABSTRACT

With the development of satellite and remote sensing techniques, more and more multi-temporal image data from airborne/satellite sensors have been collected and used in huge amounts to monitor the changes in land use and land cover. Radiometric consistency among collected multi-temporal imagery is difficult to maintain, because of variations in sensor characteristics, atmospheric conditions, solar angle, and sensor view angle. Radiometric corrections are used to remove the effects that alter the spectral characteristics of land features, except for actual changes in ground target, becoming mandatory in multi-sensor, multi-date studies. In this paper, a comparative analysis of radiometric correction of satellite images is made between Kalman filter and Levenberg algorithm. In first phase, the satellite images such as Landsat, Liss-3 have been corrected using Kalman filter technique. In the second phase, by using Levenberg algorithm radiometric correction has been performed. After that comparative study is made between the results of both techniques using different performance measures such as completeness, correctness and quality.

**Keywords:** Satellite Image, Radiometric Correction, Kalman Filter, Levenberg Algorithm, prediction.

## 1 Introduction

Nowadays satellite and airborne remote sensing system provides an enormous amount of data which are invaluable in monitoring Earth resources and the effects of human activities [2] [3] and [4]. Remote sensing is used to analyze the information about a target or an area or a phenomenon that are obtained through the remote sensor [5]. One of the advantages of remote sensing is that the measurements can be made from a large distance of about several hundred to thousand kilometers, which means that large areas on ground can be covered easily [6].

Satellite remote sensing data can provide a complement or even alternative to ground-based research for large scale studies or over long periods and is an invaluable tool for scientists, governments and the military [7] [8]. Images obtained by satellites are widely used in many environmental applications such as tracking of earth resources, geographical mapping, prediction of agricultural crops, urban growth, weather, flood and fire control etc. Space image application includes recognition and analysis of objects in the images, obtained from deep space-probe missions [9].

Satellite imaging systems like Landsat, Ikonos, QuickBird, OrbView-3, etc. has been used to collect and downlink large quantities of data [6, 8, and 9]. Images obtained through these satellites are subjected to several factors such as launch shock, loss of moisture due to vacuum, and gravity release, which will cause the values of the geometric calibration parameters to vary between the time of ground calibration and on-orbit operation [12]. Satellite image characteristics vary from date to date [8], and radiometric inconsistency among ground targets in multi-temporal imagery is produced due to the changes in sensor characteristics, atmospheric condition, solar angle, and sensor view angle [14]. Additional variation is caused by atmospheric conditions at the time of imaging, due to haze the image can be scattered at different wavelengths [8].

Therefore, radiometric corrections are performed on the raw digital image data to correct for brightness values, of the object on the ground, that have been distorted because of sensor calibration or sensor malfunction problems [13]. Radiometric corrections are classified into two types; they are absolute correction and relative corrections. Absolute radiometric correction is used to extract the absolute reflectance of scene targets at the surface of the earth and relative radiometric correction is used to reduce atmospheric and other unexpected variation among multiple images by adjusting the radiometric properties of target images to match a base image [14].

The structure of the paper is organized as follows: A brief review of the researches related to the radiometric correction is given in Section 2. The proposed comparative study of radiometric correction technique on satellite images is given in section 3. The experimental results of the proposed approach are presented in Section 4. Finally, the conclusions are given in Section 5.

## 2 Related Work

Some of the recent research works on radiometric correction of satellite images are briefly reviewed here.

In 2006, Leonardo Paolini *et al.*, [15] have discussed the effects of two types of radiometric correction methods (absolute and relative) for the determination of land cover changes, using Landsat TM and Landsat ETM+ images. In addition, they have presented an improvement to

make the relative correction method addressed. Absolute correction include a cross calibration between TM and ETM+ images, and the application of an atmospheric correction protocol. Relative correction was used to normalize the images using pseudo-invariant features (PIFs) selected through band-to-band PCA analysis. They have used an algorithm for PIFs selection, in order to improve normalization results. A post-correction evaluation index (Quadratic Difference Index (QD)), and post-classification and change detection results were used to evaluate the performance of their method. Their method has shown good post correction and post-classification results for all the images have been used (QD index < 0; overall accuracy .80%; kappa .0.65).

In 2006, Todd A. Schroeder *et al.*, [16] have presented a comparison of five atmospheric correction methods (2 relative, 3 absolute) used to correct a nearly continuous 20-year Landsat TM/ETM+ image data set (19-images) covering western Oregon (path/row 46/29). In theory, full absolute correction of individual images in a time-series have minimized the atmospheric effects resulted in a series of images that appeared more similar in spectral response than the same set of uncorrected images. To contradict that theory, they have demonstrated absolute correction methods such as Second Simulation of the Satellite Signal in the Solar Spectrum (6 s), Modified Dense Dark Vegetation (MDDV), and Dark Object Subtraction (DOS). The relative methods were the variants of an approach called absolute-normalization. This method was used to match the images in a time-series to an atmospherically corrected reference image using pseudo-invariant features and reduced major axis (RMA) regression. An advantage of “absolute-normalization” was that all images in the time-series were converted to units of surface reflectance while simultaneously being corrected for atmospheric effects. Of the two relative correction methods used for “absolute-normalization”, the first employed an automated ordination algorithm called multivariate alteration detection (MAD) to statistically locate pseudo-invariant pixels between each subject and reference image, while the second used analyst selected pseudo-invariant features (PIF) common to the entire image set. Overall, relative correction has been employed in the “absolute-normalization” context to produce the most consistent temporal reflectance response, with the automated MAD algorithm and handpicked PIFs. The “absolute normalization” scheme has improved (i.e., reduces scatter in) the spectral reflectance trajectory models used for characterizing patterns of early forest succession.

In 2008, Mahmoud El Hajj *et al.*, [17] have discussed the relative radiometric normalization for atmospheric correction. They have developed an automatic method for relative radiometric normalization based on calculating linear regressions between un-normalized and reference images. Regressions were obtained using the reflectance of automatically selected invariant targets. They have compared their method with a 6S model based atmospheric correction method. The performances of both methods were compared using 18 images from of a SPOT 5 time series acquired over Reunion Island. The results obtained for a set of manually selected invariant targets showed an excellent agreement between the two methods in all spectral

bands: values of the coefficient of determination ( $r^2$ ) exceed 0.960, and bias magnitude values were less than 2.65. Also there have been a strong correlation between normalized NDVI values of sugarcane fields ( $r^2 = 0.959$ ). Despite a relative error of 12.66% between values, very comparable NDVI patterns were observed.

In 2009, Wadii Boulila *et al.*, [7] have discussed the problem of tracking spatiotemporal changes of a satellite image through the use of Knowledge Discovery in Database (KDD). They have used prediction and decision models to discover the interesting knowledge of a given user effectively. The main objective of their work was using different KDD methods to discover knowledge in satellite image databases. Each method presented a different point of view of spatiotemporal evolution of a query model (which represents an extracted object from a satellite image). In order to combine those methods, they have used the evidence fusion theory to improve the spatiotemporal knowledge discovery process and increase the spatiotemporal model change. The experimental results of satellite images represented the region of Auckland in New Zealand depict the improvement in the overall change detection when compared to using classical methods.

In 2010, Andrea Baraldi *et al.*, [18] have analyzed the operational performance of existing stratified non-Lambertian (anisotropic) topographic correction (SNLTOC) algorithms which had been limited by the need for a priori knowledge of structural landscape characteristics, such as surface roughness. To overcome the circular nature of the SNLTOC problem, a mutually exclusive and totally exhaustive land covers classification map of a space borne MS image was required before SNLTOC takes place. Thus in their work, two methods were cascaded such as an automatic stratification at first stage and a second-stage ordinary SNLTOC method. The former has combined four sub symbolic digital-elevation-model-derived strata, namely, horizontal areas, self-shadows, and sunlit slopes either facing the sun or facing away from the sun, and 2) symbolic (semantic) strata generated from the input MS image by an operational fully automated spectral-rule-based decision-tree preliminary classifier. In this work, previous works related to the TOC subject were surveyed, and next, the operational two-stage SNLTOC system was presented. Finally, the original two-stage SNLTOC system was validated up to 19 experiments where the system's capability of reducing within-stratum spectral variance while preserving pixel-based spectral patterns (shapes) was assessed quantitatively.

In 2011, Priti Tyagi *et al.*, [1] presented eight methods for atmospheric correction in spatial domain and transform domain. They proposed atmospheric correction using linear regression model based on the wavelet transform and fourier transform. They were tested on landsat images and their performance was evaluated using visual and statistical measures. The application of the atmospheric correction methods for vegetation analyses using NDVI was also presented in the paper. Atmospheric correction using Radon Regression was also presented by the author [22] for radiometric correction of multispectral Image.

### 3 Radiometric Correction By Means of Kalman Filter and Levenberg Algorithm

Over the last few years, the satellite image analysis has played a significant role in environmental monitoring and modeling. Frequent observation of a given area over time yields the potential for several forms of change detection analysis. This radiometric inconsistency is formed due to the changes in sensor calibration, differences in illumination and observation angles, and variation in atmospheric effects [Janzen et al]. This type of deformity in satellite images should be corrected to allow for metric analyses and also adjustments may need to be applied to correct the non-homogeneous contrasts and tonal differences between adjacent frames. Thus in our research work, we have performed the radiometric correction on aerial images using two efficient methods. The proposed technique carries out in two phases. In the first phase kalman filter is applied to the remotely sensed data for obtaining predict and update state values of noisy image. In the second phase the radiometric correction on satellite images can be obtained by using Levenberg algorithm. Finally a comparison performed between corrected images resulting from both techniques. The flow diagram of the proposed scheme is given below:

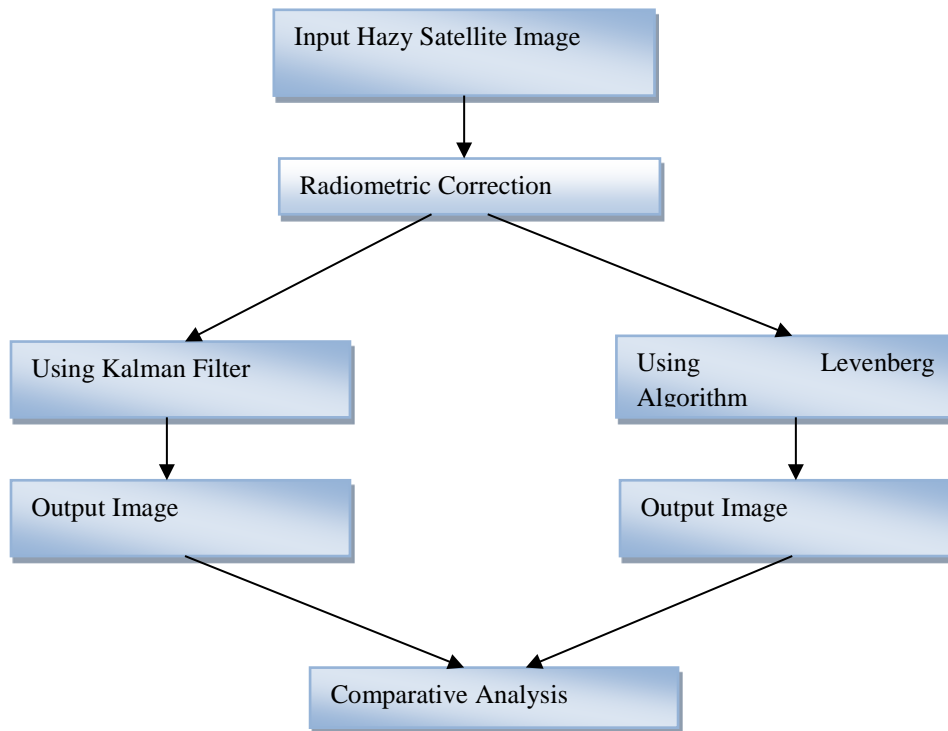


Fig 1: Flow Diagram of the proposed method

#### 3.1 Radiometric Correction Using Kalman Filter:

In 1960, Kalman filter concept has been introduced by R.E. Kalman to find the recursive solution for the discrete-data linear filtering problem. The Kalman filter is a set of mathematical equations, which offers an efficient computational (recursive) way to calculate the state of a

process, in a way that reduces the mean squared error. The filter is utilized to support the estimation of past, present, and even future states, when the precise nature of the modeled system is unknown. The Kalman filter algorithm has been implemented by two-step process, named as prediction step and update step. In the prediction stage, the Kalman filter produces estimates of the present state variables, along with their uncertainties. In the update stage, when the result of the next measurement (inevitably corrupted with some amount of error, including random noise) is observed, those estimates are updated by a weighted average, with more weight being given to estimates with higher certainty.

In steady state, the Kalman approach to radiometric correction of satellite images is depicted by the following equations,

$$x_k = Ax_{k-1} + w_{k-1} \quad (1)$$

Where,  $x_k$  is the current state vector, which contains set of variables to represent the whole system at time instant  $k$ . Also the value of  $x_k$  depends on the state transition model  $A$  applied to previous state value  $x_{k-1}$  and previous state noise  $w_{k-1}$ .

The measurement vector  $y_k$  according to the current state vector  $x_k$  applied to measurement model  $B$  and the measurement noise  $z_k$  is given as,

$$y_k = Bx_k + z_k \quad (2)$$

The random variables of state noise and measurement noise are represented as  $\{w_k\}$ ,  $\{z_k\}$  and also the error covariance of state noise and measurement noise is given in equation (3)

$$\begin{aligned} E[w_k w_l] &= Q_{kl} & p(w_k) &\sim N(0, Q) \\ E[z_k z_l] &= R_{kl} & p(z_k) &\sim N(0, R) \end{aligned} \quad (3)$$

### 3.1.1 Prediction

The Kalman filter estimates the state at time instant  $k$  and subsequently, it obtains the feedbacks in terms of noisy measurements.

Predicted (a priori) state estimate is,

$$\hat{x}_{k/k-1} = A\hat{x}_{k-1/k-1} \quad (4)$$

Predicted (a priori) estimate covariance is,

$$P_{k/k-1} = AP_{k-1/k-1}A^T + Q \quad (5)$$

### 3.1.2 Updating

Kalman gain is given as,

$$K_k = P_{k/k-1} B_k^T [D_k]^{-1} \tag{6}$$

Where,  $D_k = B_k P_{k/k-1} B_k^T + R$

Updated (a posteriori) state estimate and updated (a posteriori) estimate covariance is given in the following equations:

$$\hat{x}_{k/k} = \hat{x}_{k/k-1} + K_k (y_k - B_k \hat{x}_{k/k-1}) \tag{7}$$

$$P_{k/k} = [I - K_k B_k] P_{k/k-1} \tag{8}$$

### 3.2 Radiometric correction using Levenberg Marquardt (LM) Algorithm:

The Levenberg-Marquardt (LM) algorithm is the most extensively utilized optimization algorithm [20]. It outperforms simple gradient descent and other conjugate gradient methods in a wide variety of problems. It is the most prominent curve-fitting algorithm used in numerous software applications for solving generic curve-fitting problems. Here, the problem is the radiometric inconsistency of the satellite images. Given a set of  $n$  data pairs of independent and dependent variables  $(x_i, y_i)$ , and optimize the parameters  $\beta$  of the model curve so that, the minimal function  $R(\beta)$  is given as,

$$R(\beta) = \sum_{i=1}^n [y_i - f(x_i, \beta)]^2 \tag{9}$$

Steps involved in Levenberg Marquardt (LM) Algorithm:

(i) To begin the iterative procedure of the Levenberg Marquardt algorithm for minimization, the user has to assume the value for parameter vector  $\beta$ .

(ii) In each iteration, the parameter vector  $\beta$  is replaced by a new estimate  $\beta + \delta$

(iii) To find  $\delta$ , the functions  $f(x_i, \beta + \delta)$  are approximated by their linearizations  $f(x_i, \beta + \delta) \approx f(x_i, \beta) + J_i \delta$

Where  $J_i$  is the gradient of  $f$  with respect to  $\beta$  and is given by,  $J_i = \frac{\partial f(x_i, \beta)}{\partial \beta}$

(iv) To determine the minimum of the sum of squares  $R(\beta)$ , the gradient of  $R$  with respect to  $\delta$  will be zero. The above first-order approximation of  $f(x_i, \beta + \delta)$  is given as,

$$R(\beta + \delta) \approx \sum_{i=1}^n (y_i - f(x_i, \beta) - J_i \delta)^2 \tag{10}$$

(v) Taking the derivative with respect to  $\delta$  and setting the result to zero gives

$$(J^T J) \delta = J^T [y - f(\beta)] \tag{11}$$

Where  $J$  is the Jacobian matrix,  $y$  and  $f$  are the vectors containing elements  $y_i$ ,  $f(x_i, \beta)$  respectively.

(vi) By Levenberg's contribution, the above equation is replaced by a "damped version", which is represented as,

$$(J^T J + \lambda I) \delta = J^T [y - f(\beta)] \quad (12)$$

Where  $I$  is the Identity matrix, giving as the increment  $\delta$  to the parameter vector  $\beta$  and the non negative factor  $\lambda$  is adjusted for each iteration.

(vii) The drawback of Levenberg's algorithm is, if the value of damping factor  $\lambda$  is large, then inverting  $J^T J + \lambda I$  becomes tricky. Thus Marquardt replaced the identity matrix  $I$  with the diagonal matrix consisting of the diagonal elements  $J^T J$ . Thus the resulting Levenberg–Marquardt algorithm is,

$$(J^T J + \lambda \text{diag}(J^T J)) \delta = J^T [y - f(\beta)] \quad (13)$$

## 4 Experimental Data and Results

The proposed comparative study of radiometric correction using both techniques was done in the working platform of MATLAB.

### 4.1 Experimental Data:

The satellite images used in the proposed work are obtained from LISS-III and Landsat 7 ETM+ sensors which are given in Fig 2. A LISS-III satellite image acquired in March 2, 2006 is shown in fig 2(a) and a Landsat 7 ETM+ image acquired in March 2000 to show the region of San Francisco is shown in fig 2(b). The sensor specifications such as band type, resolution, wavelength and description of each band of input Landsat 7 ETM+ image is detailed in Table 1.

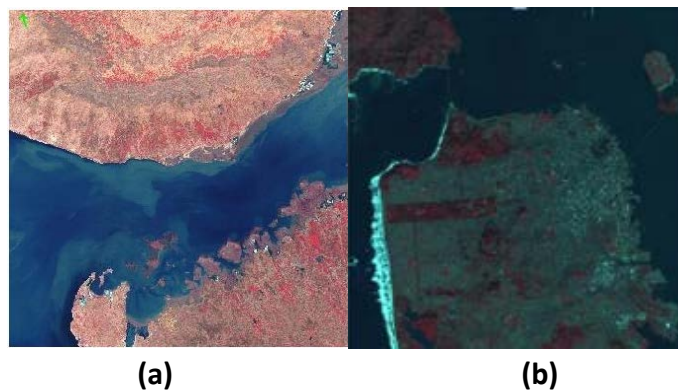


Fig 2: Input Images, a) LISS-III satellite image, b) Landsat ETM+ satellite image

**Table 1: Landsat ETM+ sensor specifications**

Band	Resolution( <i>m</i> )	Wavelength( $\mu m$ )	Description
1	30m	0.45-0.52	Blue
2	30m	0.52-0.60	Green
3	30m	0.63-0.69	Red
4	30m	0.76-0.90	Near Infrared
5	30m	1.55-1.75	Short-wave Infrared
6	60m	10.4-12.5	Thermal Infrared
7	30m	2.09-2.35	Short-wave Infrared
8	15m	0.45-0.80	Panchromatic

## 4.2 Results and Analysis:

The experiments have been conducted on the input LISS-III and Landsat 7 ETM+ satellite images using Kalman filter and Levenberg-Marquardt (LM) algorithm. Fig 3 illustrates the resultant of both satellite images obtained using Kalman filter and Fig 4 shows the output images obtained by using Levenberg-Marquardt (LM) algorithm.

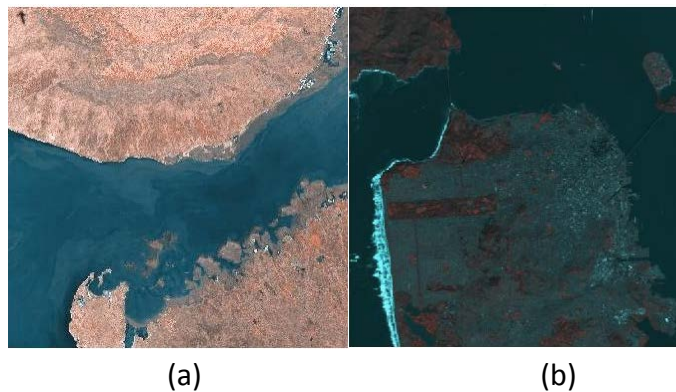


**Fig 3: Radiometric corrected output using Kalman filter for (a) LISS-III satellite image (b) Landsat 7 ETM+ satellite image.**



(a) (b)

**Fig 4: Radiometric corrected output using Levenberg-Marquardt (LM) algorithm for (a) LISS-III satellite image (b) Landsat 7 ETM+ satellite image.**

Our proposed method improves the quality of remote sensing data by means of Kalman filter and Levenberg-Marquardt (LM) algorithm. Different quality measures such as Peak Signal to Noise Ratio, Mean Square Error and Root Mean Square Error has been calculated for both methods and is given in Table 2, and 3.

As per Table 2, by using the Kalman filter for radiometric correction on LISS-III satellite image, obtained PSNR, MSE and RMSE values are +27.73091 dB, 331.52031 and 18.20770 respectively. While using the same filter for Landsat image, PSNR, MSE and RMSE values are +31.85306 dB, 128.32016 and 11.32785 respectively. Table 3 illustrates the quality measurements (PSNR, MSE, and RMSE) of both satellite images using Levenberg-Marquardt (LM) algorithm. For LISS-III image, PSNR, MSE and RMSE values are +17.86615 dB, 3213.55751 and 56.6882. For Landsat image, PSNR, MSE and RMSE values are +27.22954 dB, 372.08957 and 19.28962 respectively. Table 4 illustrates the comparison results of Kalman filter and Levenberg-Marquardt (LM) algorithm for LISS-III and Landsat 7 ETM+ satellite images respectively.

**Table 2: Quality Metrics of LISS-III and Landsat ETM+ satellite images Using Kalman filter**

Quality Metrics	LISS-III satellite Image	Landsat 7 ETM+ satellite Image
PSNR	+27.73091 dB	+31.85306 dB
MSE	331.52031	128.32016
RMSE	18.20770	11.32785

**Table 3: Quality Metrics of LISS-III and Landsat ETM+ satellite images Using Levenberg-Marquardt (LM) algorithm**

Quality Metrics	LISS-III satellite Image	Landsat 7 ETM+ satellite Image
PSNR	+17.86615 dB	+27.22954 dB
MSE	3213.55751	372.08957

RMSE	56.6882	19.28962
------	---------	----------

Table 4: Quality Metrics Comparison Results

Quality Metrics	LISS-III satellite Image		Landsat 7 ETM+ satellite Image	
	Kalman filter	Levenberg-Marquardt	Kalman filter	Levenberg-Marquardt
PSNR	+27.73091 dB	+17.86615 dB	+31.85306 dB	+27.22954 dB
MSE	331.52031	3213.55751	128.32016	372.08957
RMSE	18.20770	56.6882	11.32785	19.28962

From the values represented in Table 4, it can be seen that for LISS-III satellite image, the PSNR value of Kalman filter output is higher than Levenberg-Marquardt output. According to the MSE and RMSE values, the Kalman filter output is low when compared to the Levenberg-Marquardt algorithm output. Also, for Landsat 7 ETM+ satellite image the PSNR value of Kalman filter output is greater than Levenberg-Marquardt method. The MSE and RMSE values of Kalman filter output is relatively low when compared with the Levenberg-Marquardt algorithm output. By comparing PSNR, MSE and RMSE values from the above table, it is shown that the radiometric correction performance of Kalman filter is relatively high for both types of satellite images.

## 5 Conclusion

In this paper, comparative analysis of radiometric correction on different types of satellite images was made using two efficient techniques such as Kalman filter and Levenberg-Marquardt algorithm. First of all, Kalman filter has been utilized for radiometric correction on remote sensing data and after that Levenberg-Marquardt algorithm has been used for the same process. The study helped to analyze the performance of both methods for radiometric correction on different satellite images by means quality parameters such as peak signal to noise ratio, mean square error and root mean square error. From the experimental results, we can conclude that Kalman filter works in a better way to perform the radiometric correction on different satellite images.

## REFERENCES

- [1] Priti Tyagi, Udhav Bhosle, "Atmospheric correction of Remotely sensed Images in Spatial and Transform Domain", International Journal of Image Processing, Vol(5), Issue (5), pp 564-579, 2011

- [2] Seema Biday, and Udhav Bhosle, "Relative Radiometric Correction of Cloudy Multitemporal Satellite Imagery", *International Journal of Civil and Environmental Engineering*, Vol.2, No.3, 2010.
- [3] Mirnalinee Dhinesh, Sukhendu Das and Koshy Varghese, "Automatic Curvilinear Structure detection from Satellite Images using Multiresolution GMM ", *International Journal of Imaging Science and Engineering (IJISE)*, Vol.2, No.1, pp. 154-157, 2008.
- [4] Michael Schroder, Hubert Rehrauer, Klaus Seidel, and Mihai Datcu, "Spatial Information Retrieval from Remote-Sensing Images—Part II: Gibbs–Markov Random Fields", *IEEE Transactions on geoscience and remote sensing*, Vol. 36, No. 5, pp.1446-1455, 1998.
- [5] T Rajani Mangala and S G Bhirud, "An Effective ANN-Based Classification System for Rural Road Extraction in Satellite Imagery", *European Journal of Scientific Research*, Vol.47, No.4, pp.574-585, 2010.
- [6] Rajiv Kumar Nath and S K Deb, "Water-Body Area Extraction from High Resolution Satellite Images-An Introduction, Review, and Comparison", *International Journal of Image Processing (IJIP)*, Vol. 3, No.6, pp.353-372, 2010.
- [7] Wadii Boulila, Imed Riadh Farah, Karim Saheb Ettaba, Basel Solaiman, and Henda Ben Ghezala, "Improving Spatiotemporal Change Detection: A High Level Fusion Approach for Discovering Uncertain Knowledge from Satellite Image Databases", *World Academy of Science, Engineering and Technology*, Vol. 52, No.12, pp 52-57, 2009.
- [8] Sarah C. Goslee, "Analyzing Remote Sensing Data in R: The landsat Package", *Journal of Statistical Software*, Vol. 43, No.4, pp.1-25, 2011.
- [9] Salem Saleh Al-amri, N.V. Kalyankar and Khamitkar S.D, "A Comparative Study of Removal Noise from Remote Sensing Image", *IJCSI International Journal of Computer Science Issues*, Vol. 7, No. 1, pp. 32-36, 2010.
- [10] Ellison, J. and Milstein, J, "Improved Reduced-Resolution Satellite Imagery", In *proceedings of Goddard Conf. on Space Applications of Artificial Intelligence & Emerging Info. Technologies* in Los Angeles, CA, 9-11 May 1995, pp. 163-178.
- [11] H. Liu, J. Li and M. A. Chapman, "Automated Road Extraction from Satellite Imagery Using Hybrid Genetic Algorithms and Cluster Analysis", *Journal of Environmental Informatics*, Vol.1, No.2, pp.40-47, 2003.
- [12] David Mulawa, "On-Orbit Geometric Calibration Of The Orbview-3 High Resolution Imaging Satellite", In *proceedings of the XXth International Society for Photogrammetry and Remote Sensing Congress (ISPRS)*, 2004.
- [13] S.Santhosh Baboo and M.Renuka Devi, "Geometric Correction in Recent High Resolution Satellite Imagery: A Case Study in Coimbatore, Tamil Nadu", *International Journal of Computer Applications*, Vol. 14, No.1, pp.32-37, 2011.

- [14] Xuexia Chena, Lee Vierlinga, and Don Deering, "A simple and effective radiometric correction method to improve landscape change detection across sensors and across time", *Remote Sensing of Environment Journal*, Vol. 98, No.1, pp.63–79, 2005.
- [15] Leonardo Paolini, Francisco Grings, Jose A. Sobrino, Juan C. Jime Nez Munoz and Haydee karszenbaum, "Radiometric correction effects in Landsat multi-date/multi-sensor change detection studies", *International Journal of Remote Sensing*, Vol. 27, No.4, pp.685–704, 2006.
- [16] T Schroeder, W Cohen, C Song, M Canty, and Z Yang, "Radiometric correction of multi-temporal Landsat data for characterization of early successional forest patterns in western Oregon", *Remote Sensing of Environment Journal*, Vol.103, No.1, pp. 685–704, 2006.
- [17] M. El Hajj , A. Begue , B. Lafrance , O. Hagolle , G. Dedieu , and M. Rumeau, "Relative radiometric normalization and atmospheric correction of a SPOT 5 time series", *Sensors Journal*, Vol.8, pp.2774 – 2791, 2008.
- [18] Andrea Baraldi, Matteo Gironda, and Dario Simonetti, "Operational Two-Stage Stratified Topographic Correction of Spaceborne Multispectral Imagery Employing an Automatic Spectral-Rule-Based Decision-Tree Preliminary Classifier", *IEEE transactions on geoscience and remote sensing*, Vol. 48, No. 1, pp.112-146, 2010.
- [19] Darren T. Janzen, Arthur L. Fredeen, and Roger D. Wheate, "Radiometric correction techniques and accuracy assessment for Landsat TM data in remote forested regions", *Can. J. Remote Sensing*, Vol. 32, No. 5, pp. 330–340, 2006.
- [20] R. E. Kalman, "A New Approach to Linear Filtering and Prediction Problems", *Journal of Basic Engineering*, Vol.82 (Series D), pp.35-45, 1960.
- [21] K. Levenberg, "A method for the solution of certain non-linear problems in least squares", *Quarterly Journal of Applied Mathematics*, Vol. II, No.22, pp.164--168,1944.
- [22] Priti Tyagi, Udhav Bhosle, "Radiometric correction of Multispectral Images using Radon Transform", *Journal of Indian Society of Remote Sensing*, DOI 10.1007/s12524-013-0307-y, 2013